ORIGINAL SCIENTIFIC PAPER

CROATICA CHEMICA ACTA

*Croat. Chem. Acta* **2016**, *89*(4), 535–541
Published online: April 9, 2017
DOI: 10.5562/cca3026

HKD 1926

# Structural and Antioxidative Features of Chlorogenic Acid

Jelena Tošović,* Svetlana Marković

University of Kragujevac, Faculty of Science, Radoja Domanovića 12, 34000 Kragujevac, Serbia
* Corresponding author's e-mail address: jelena.tosovic@kg.ac.rs

RECEIVED: October 11, 2016 * REVISED: February 28, 2017 * ACCEPTED: March 1, 2017

PROCEEDING OF THE 28TH MATH/CHEM/COMP CONFERENCE, JUNE 20–25, 2016, DUBROVNIK, CROATIA

**Abstract:** This work contributes to the structure clarification of chlorogenic acid (5-*O*-caffeoylquinic acid, **5CQA**) by comparing the experimental and simulated IR, Raman, $^{1}$H-NMR, $^{13}$C-NMR, and UV-vis spectra. The lowest-energy conformers in the gas-phase and solution were used for all calculations. Very good agreement between all experimental and simulated spectra indicates correct arrangement of the atoms in the **5CQA** molecule. In addition, the bond dissociation enthalpies, proton affinities, electron transfer enthalpies, ionization potentials, and proton dissociation enthalpies for **5CQA** were used for thermodynamic consideration of the major antioxidative mechanisms: HAT (Hydrogen Atom Transfer), SPLET (Sequential Proton-Loss Electron-Transfer), and SET-PT (Single Electron Transfer – Proton Transfer). It was found that HAT may be the predominant mechanism in nonpolar solvents, while HAT and SPLET are competitive pathways in polar media.

All quantum-chemical calculations were carried out by means of the MN12-SX method. Its performance is similar to those of the B3LYP-D2, B3LYP-D3, and M06-2X functionals.

**Keywords**: chlorogenic acid, spectral properties, thermodynamic parameters, MN12-SX.

## INTRODUCTION

CHLOROGENIC acid (5-*O*-caffeoylquinic acid, **5CQA**), an ester formed between caffeic and quinic acids (Figure 1), is a natural polyphenol that can be isolated from various fruits and vegetables. This compound is an important secondary metabolite with various roles in plants. It has been demonstrated that enhanced levels of **5CQA** in transgenic tomato plants improve protection from the UV radiation, and increase microbial resistance.[1,2] In addition, it has been shown that **5CQA** acts as pest resistance factor in ornamental plants.[3] Like other dietary polyphenols, **5CQA** shows pharmacological and biological activities such as antihypertensive, antitumor, antidiabetic, hypo-lipidemic, and anti-inflammatory, as well as antioxidative properties.[4–10] Polyphenols realize their antioxidative action via several mechanisms: hydrogen atom transfer (HAT), sequential proton loss electron transfer (SPLET), single electron transfer – proton transfer (SET-PT), proton coupled electron transfer (PCET), radical adduct formation (RAF), single electron transfer (SET), and sequential proton loss hydrogen atom transfer (SPLHAT).[11–14] However, HAT (eq. 1), SPLET (eqs 2 and 3), and SET-PT (eqs 4 and 5) are considered as major antioxidative mechanisms, as they are most often obeyed by various polyphenols.

$$\mathrm{ArOH} \rightarrow \mathrm{ArO}^{\bullet} + \mathrm{H}^{\bullet} \quad (1)$$

$$\mathrm{ArOH} \rightarrow \mathrm{ArO}^{-} + \mathrm{H}^{+} \quad (2)$$

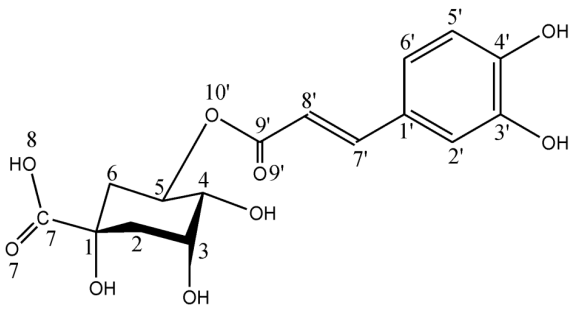


**Figure 1.** Atom labelling scheme in chlorogenic acid (**5CQA**).

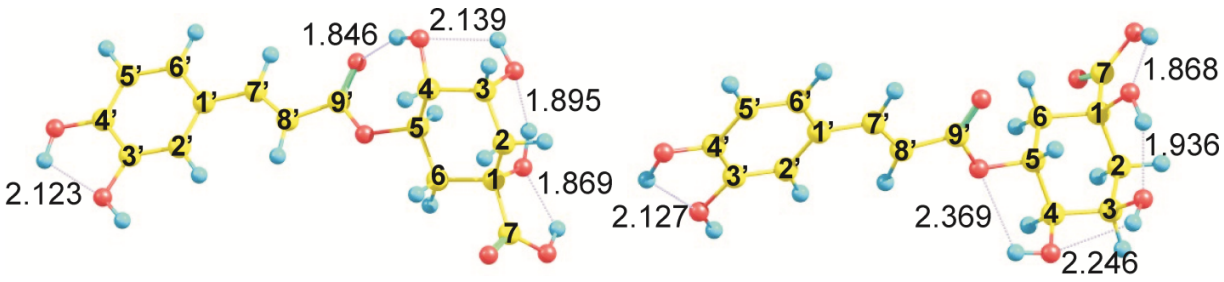


**Figure 2.** Gas-phase (left) and solvated (right) structures of chlorogenic acid. The hydrogen bond lengths are given in Å.

$$ArO^- \rightarrow ArO^{\bullet} + e^- \quad (3)$$

$$ArOH \rightarrow ArO^{+\bullet} + e^- \quad (4)$$

$$ArOH^{+\bullet} \rightarrow ArO^{\bullet} + H^+ \quad (5)$$

In the reactions (1)–(5) $ArO^{\bullet}$, $ArO^-$, and $ArOH^{+\bullet}$ represent the free radical, anion, and radical cation of the phenolic compound ArOH. The corresponding reaction enthalpies are called: bond dissociation enthalpy (BDE), proton affinity (PA), electron transfer enthalpy (ETE), ionization potential (IP), and proton dissociation enthalpy (PDE), respectively.

**5CQA** is a white powder for which the X-ray powder diffraction has not been carried out. So, its structural features have not been completely elucidated. There are few experimental studies dedicated to the NMR and Raman spectra of **5CQA**.[15–18] A preferential conformation of **5CQA** in methanol solution has recently been determined on the basis of the $^1$H-NMR, $^{13}$C-NMR, DQF-COSY, z-filtered TOCSY, ROESY, phase-sensitive HMBC, and HSQC experiments.[17] UV-vis absorption spectroscopy has been used to investigate complex formation of some metal ions with **5CQA**.[19,20] In our recent work, we used different spectroscopic methods (IR, Raman, UV-vis, $^1$H- and $^{13}$C-NMR) in order to contribute to clarification of the **5CQA** structure.[21] In addition, we performed a comprehensive study of the antioxidative activity of **5CQA** by focusing on the thermodynamics of the three major antioxidative mechanisms: HAT, SPLET, and SET-PT. It was shown that HAT may be the predominant mechanism in nonpolar solvents, while HAT and SPLET are competitive pathways in polar media.[22]

All these tasks were realized by performing necessary quantum chemical calculations at the B3LYP-D2, B3LYP-D3 and M06-2X levels of theory. It is well-known that numerous density functionals are nowadays available. In this work we focus our attention towards the MN12-SX method. This method is a screened exchange hybrid meta-NGA (nonseparable gradient approximation) functional that uses a finite amount of the Hartree-Fock (HF) exchange at short-range, and none in the large-range limit.[23] The aim of this approximation is to reduce high computational costs resulting from the HF exchange. Our aim is to examine its performance in the investigations devoted to the spectral and antioxidative properties of **5CQA**. Our additional goal is to carry out a comparison of the results obtained with different density functionals.

## MATERIALS AND METHODS

The vibrational spectra, NMR spectra in DMSO-d6 with TMS as the internal standard, and UV-vis spectrum in methanol of **5CQA** were recorded in a manner described in our related work.[21] There, a detailed conformational analysis of **5CQA** has been performed using the gas-state B3LYP/6-31G(d) calculations. Twenty conformers of the lowest total energy have been reoptimized in the gas-state and solution using the B3LYP-D2, B3LYP-D3 and M06-2X functionals in combination with the 6-311+G(d,p) and 6-311++G(d,p) basis sets.[21,22] In the present work we used the MN12-SX/6-311+G(d,p) theoretical model to reoptimize the same twenty conformers of **5CQA**. The calculations revealed the gas-phase geometries, as well as those in the DMSO (dielectric constant $\varepsilon$ = 46.8260) and methanol ($\varepsilon$ = 32.6130) solutions. These solvents were selected to mimic the conditions of experimental measurements, and their influence was taken into account by applying the CPCM polarizable continuum solvation model.[24] Frequency calculations were included; there were no imaginary frequencies. A comparison of the free energy values resulting from the four methods: B3LYP-D2, B3LYP-D3, M06-2X, and MN12-SX, revealed that there are only minor differences in the orders of conformer stability in all three media. Furthermore, the most stable conformations in the gas-phase and in both solutions for all four methods are exactly the same. The optimized geometries of the most stable conformations of **5CQA** obtained with the MN12-SX method in the gas-phase and DMSO solution are presented in Figure 2.

The gas-phase geometry of **5CQA** was used to simulate the IR and Raman spectra, while its solvated geometry was used to predict the NMR and UV-vis spectra. The vibrational modes of **5CQA** were assigned on the basis of the potential energy distribution (PED) analysis[25] using the VEDA 4 software.[26] The gauge independent atomic orbital (GIAO) method was used for prediction of the

$^{13}$C NMR and $^{1}$H properties of **5CQA** in DMSO, whereas the time dependent density functional theory (TDDFT) calculations were used for simulation of the UV-vis spectrum of this compound in methanol.

The free radicals, anions, and radical cation of **5CQA** were issued from the solvated geometry. The structures of all species in the solvents of different polarity: benzene ($\varepsilon$ = 2.2706), methanol, and water ($\varepsilon$ = 78.3553), were obtained by full optimizations and frequency calculations. Taking into account that free radicals, including hydrogen atoms, were considered, these calculations were carried out by employing the MN12-SX/6-311++G(d,p) level of theory in combination with the CPCM solvation model. The so-obtained enthalpies were used to compute the BDE, PA, ETE, IP, and PDE values, required for a description of the HAT, SPLET, and SET-PT mechanisms of **5CQA** in the three solvents.

Gaussian 09 program package was employed for all quantum chemical calculations.[27]

## RESULTS AND DISCUSSION

As in the case of B3LYP-D3 and M06-2X,[21] the MN12-SX geometries of **5CQA** in DMSO and methanol are mutually very similar. The solvated structure is in perfect agreement with the finding of Forino et al. based on a detailed NMR study.[17] This structure is characterized with the O4–H4···O10' hydrogen bond. The only significant difference of the gas-phase geometry is that it is characterized with the O4–H4···O9' hydrogen bond (Figure 2). In both structures there are very strong O8–H8···O1 and O1–H1···O3 hydrogen bonds that influence the orientation of all hydroxyl groups in the quinic moiety of **5CQA**.

### Spectroscopic and Structural Properties of Chlorogenic Acid

Due to the fact that **5CQA** possesses six hydroxyl groups, which have a significant impact on the vibrational spectra appearance, these spectra are very complex with in total

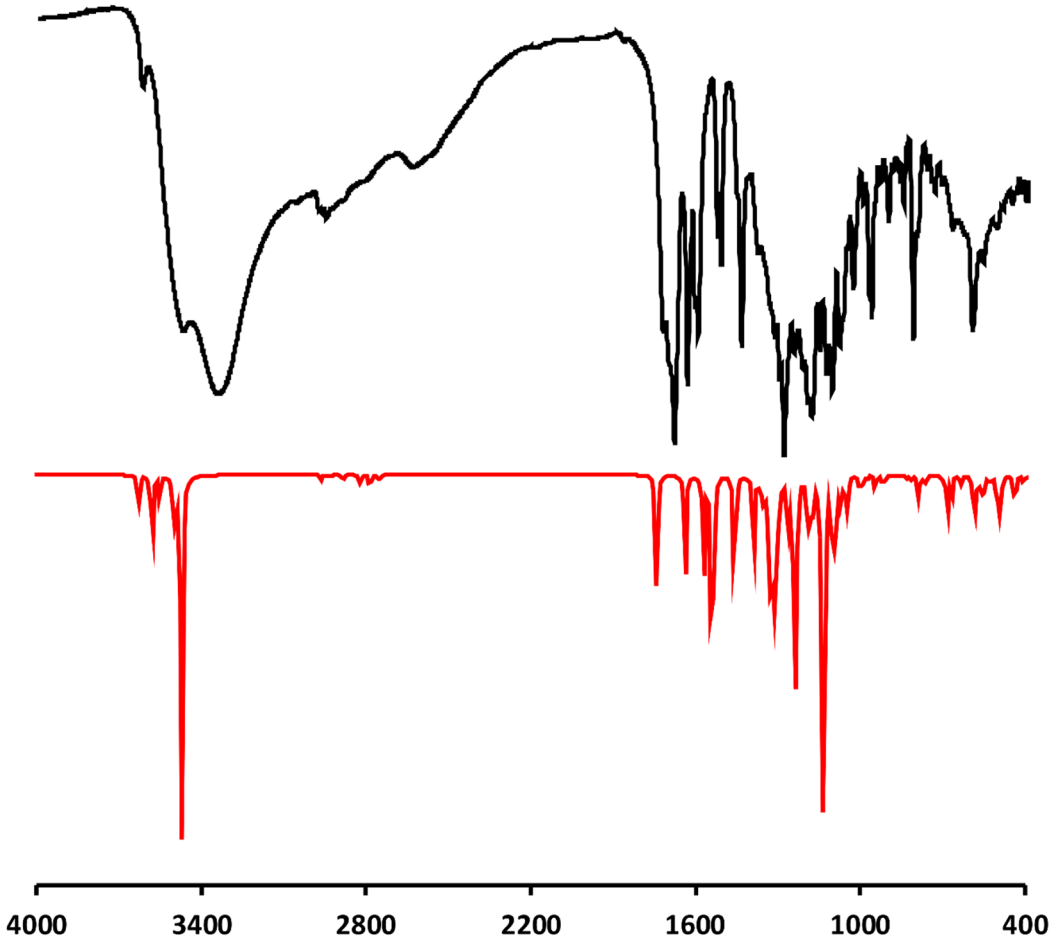


Figure 3. Experimental (black) and calculated (red) IR spectra of 5CQA.

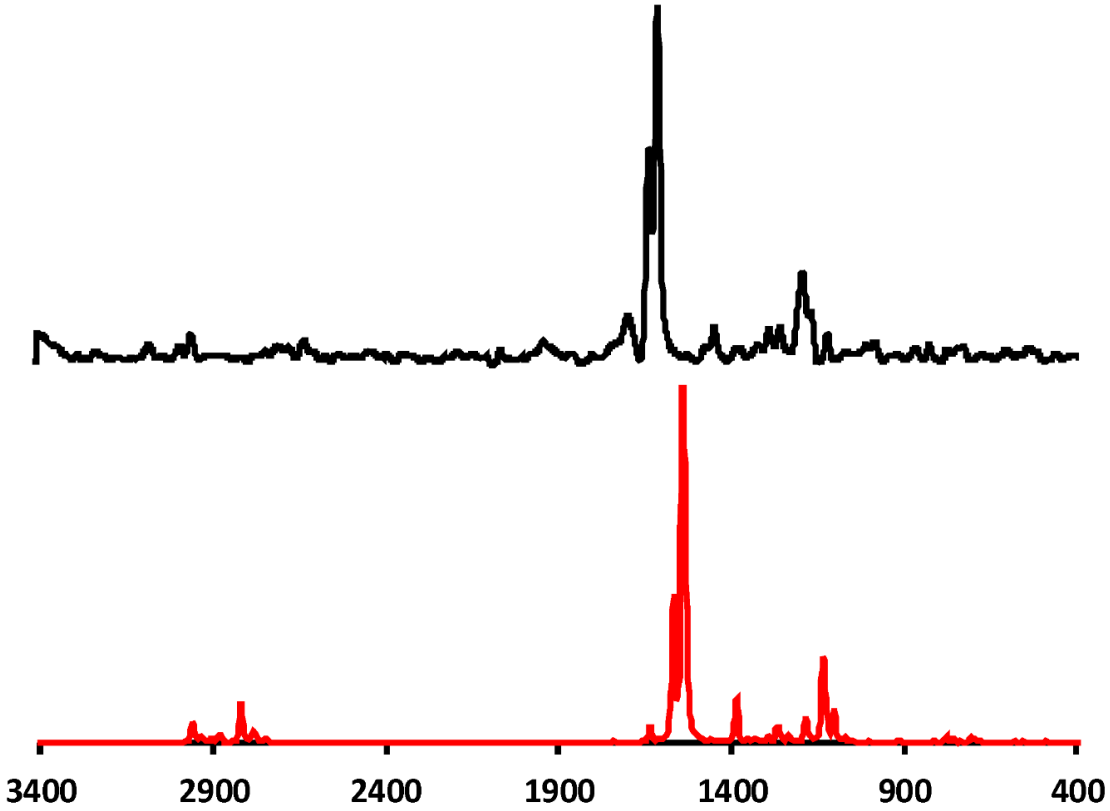


Figure 4. Experimental (black) and calculated (red) Raman spectra of 5CQA.

123 spectral modes. The vibrational scaling factors for the number of different computational methods can be found in literature. [28] However, to our best knowledge, the scaling factor for the MN12-SX/6-311+G(d,p) theoretical model has not been reported. In present study, the scaling factor for this method was determined on the basis of the experimental data for the IR spectrum using the least squares method, and it amounts to 0.923. The calculated values of the wavenumbers were scaled and assigned to the corresponding experimental values. The IR and Raman spectra of **5CQA** are depicted in Figures 3 and 4, whereas the most important vibrational modes of the compound are presented in Table 1.

The quality of the linear correlation between the experimental and calculated wavenumbers was evaluated by means of three descriptors: the correlation coefficient (R), average absolute error (AAE), and average relative error (ARE). The R value for the IR and Raman spectra are identical and amount to 0.9990. The AAE and ARE values for the IR spectrum are equal to 24.3 $cm^{-1}$ and 1.8 %, whereas for the Raman spectrum AAE and ARE amount to 23.2 $cm^{-1}$ and 1.8 %. The AAE and ARE values obtained with the MN12-SX method for both spectra are very similar to those obtained with B3LYP-D3 and M06-2X, indicating reasonable capability of the applied method to reproduce this kind of spectra. It should be pointed out that the simulated vibrational spectra refer to an isolated molecule of **5CQA**, implying that intermolecular interactions, including hydrogen bonds, are neglected. Certainly, this fact is the most important source of slight disagreement between the experimental and calculated band positions.

Very massive and intense overlapping bands in the IR spectrum, which appear in the region of 4000–2000 $cm^{-1}$, were assigned to the different modes of the O–H vibrations. The high frequency region is also characterized by the C–H stretching modes of acyclic chain and quinic moiety. The bands of the medium and strong intensities at 1732 (IR) and 1690 $cm^{-1}$ (IR) were assigned to the C–O

**Table 1.** Characteristic experimental and calculated wavenumbers (ν) in the vibrational spectra of chlorogenic acid

| Mode assignment | $\nu_{IR}$ | $\nu_{Raman}$ | MN12-SX |
|---|---|---|---|
| | Exp.[21] / cm$^{-1}$ | | Calcd. / cm$^{-1}$ |
| OH stretching (b[a]) | 3624 s[b] | | 3582 |
| OH stretching (q) | 3473 s | | 3500 |
| OH stretching (q) | 3348 s | | 3473 |
| CH stretching (a) | | 2984 w | 2963 |
| CH stretching (q) | 2953 w | 2951 w | 2929 |
| CO stretching (q) | 1732 m | | 1742 |
| CO stretching (a) | 1690 vs | 1690 w | 1638 |
| CC stretching (b, a) | 1639 vs | 1632 s | 1571 |
| CC stretching (b, a) | 1602 s | 1604 vs | 1541 |
| CC stretching (b, a) | 1443 s | 1443 m | 1389 |

[a] b, a, and q denote benzene moiety, acyclic chain, and quinic moiety, respectively

[b] vs, s, m, and w stand for very strong, strong, medium, and weak vibrations

stretching modes of the acyclic chain and quinic moiety. In addition, the bands of the medium and strong intensities at 1639 (IR), 1632 (R), 1604 (R), 1602 (IR) and 1443 cm$^{-1}$ (IR, R) were mostly assigned to the C–O stretching modes of the acyclic chain and benzene moiety.

Due to the fact that the chemical shifts in the simulated $^{13}$C-NMR spectrum were underestimated, and in the $^{1}$H-NMR spectrum were overestimated, the calculated values were scaled. As in the case of the vibrational spectra, the scaling factors were determined by means of the least squares method, and they amount to 1.066 and 0.928 for $^{13}$C-NMR and $^{1}$H-NMR. The obtained results are presented in Table 2. A comparison between the experimental and calculated chemical shifts shows that the correlation coefficients for $^{13}$C-NMR and $^{1}$H-NMR are equal to 0.997 and 0.996, whereas the AAE values are equal to 2.26 and 0.17 ppm, respectively.

**Table 2.** Experimental and calculated NMR properties of chlorogenic acid in DMSO. Chemical shifts for the $^{13}$C- and $^{1}$H-NMR spectra are given in ppm

| C | Calcd. | Exp.[21] | H | Calcd. | Exp.[21] |
|---|---|---|---|---|---|
| **7** | 172.62 | 175.07 | **7'** | 7.535 | 7.420 |
| **9'** | 164.55 | 165.89 | **2'** | 6.893 | 7.035 |
| **4'** | 148.87 | 148.50 | **6'** | 6.967 | 6.985 |
| **3'** | 142.60 | 145.73 | **5'** | 6.634 | 6.760 |
| **7'** | 149.92 | 145.10 | **8'** | 6.152 | 6.150 |
| **1'** | 124.67 | 125.78 | **5[ax]** | 4.686 | 5.060 |
| **6'** | 131.22 | 121.51 | **3[eq]** | 4.223 | 3.919 |
| **5'** | 115.67 | 115.92 | **4[ax]** | 3.729 | 3.566 |
| **8'** | 112.03 | 114.96 | **2[ax]** | 2.027 | 2.060 |
| **2'** | 110.11 | 114.49 | **6[ax]** | 1.943 | 1.983 |
| **1** | 74.05 | 73.67 | **6[eq]** | 2.293 | 1.895 |
| **4** | 71.90 | 71.04 | **2[eq]** | 2.124 | 1.775 |
| **5** | 69.30 | 70.59 | | | |
| **3** | 70.35 | 68.27 | | | |
| **6** | 37.52 | 37.39 | | | |
| **2** | 37.46 | 36.48 | | | |

By comparing the results obtained with the B3LYP-D3 and M06-2X methods[21] with the results shown in Table 2, it can be concluded that the MN12-SX functional achieves the best agreement with the experimental NMR spectra of **5CQA**. Yet, the deviation of the calculated chemical shifts from the experimental values is notable for some carbon atoms: C2', C6' and C8'. This occurrence is a consequence of facile rotation of the benzene moiety around the single C1'–C7' bond. Very good agreement between the experimental and calculated chemical shifts in the $^{1}$H-NMR spectrum indicates decreased flexibility of the quinic moiety, which is a consequence of the directed hydrogen bonds.

The experimental UV-vis spectrum of **5CQA** in methanol consists of four bands at 329, 298, 244, and 218 nm.[21] The simulated spectrum, obtained at the TDDFT/MN12-SX/6-311+G(d,p) level of theory, shows only one intensive absorption band at 328 nm. This band corresponds to a $\pi \rightarrow \pi^*$ electronic transition from the HOMO to the LUMO (Figure 5). There is a large sharing region between the HOMO and LUMO of **5CQA**, as both orbitals are delocalized over the caffeic moiety. These findings, as well as the small HOMO-LUMO gap of 0.13564 au, explain the pronounced intensity of this band. Interestingly, this analysis of the HOMO→LUMO transition, based on the Kohn-Sham orbitals, agrees very well with that based on the NLMO clusters.[29] Namely, the HOMO cluster of **5CQA** is delocalized over the caffeic moiety, whereas the LUMO cluster is delocalized over the acyclic chain (more precisely – over the C9'-O9' carbonyl group and adjacent carbon and oxygen atom).[21]

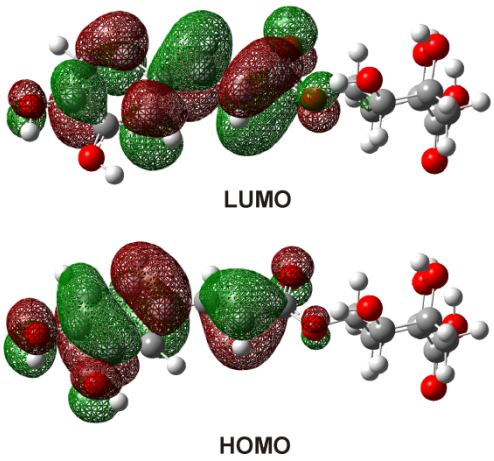


**Figure 5.** Frontier orbitals of chlorogenic acid.

Although the agreement between the calculated and experimental wavelengths of the first band is excellent, the other bands were not reproduced. While B3LYP-D3 was very successful, and M06-2X underestimated all four bands,[21] the MN12-SX functional failed to reproduce the entire UV-vis spectrum of **5CQA**.

## Antioxidative Activity of Chlorogenic Acid: Thermodynamic Approach

In order to assume which antioxidative mechanism – HAT, SPLET or SET-PT, is a predominant pathway in **5CQA**, we determined the corresponding thermodynamic parameters: BDE, PA, ETE, IP, and PDE. These parameters were calculated as the enthalpies of the reactions (1)–(5) in benzene, methanol, and water; namely:

$$\mathrm{BDE} = H(\mathrm{ArO}^{\bullet}) + H(\mathrm{H}^{\bullet}) - H(\mathrm{ArOH}) \quad (6)$$

$$\mathrm{PA} = H(\mathrm{ArO}^{-}) + H(\mathrm{H}^{+}) - H(\mathrm{ArOH}) \quad (7)$$

$$\mathrm{ETE} = H(\mathrm{ArO}^{\bullet}) + H(\mathrm{e}^{-}) - H(\mathrm{ArO}^{-}) \quad (8)$$

$$\mathrm{IP} = H(\mathrm{ArOH}^{+\bullet}) + H(\mathrm{e}^{-}) - H(\mathrm{ArOH}) \quad (9)$$

$$\mathrm{PDE} = H(\mathrm{ArO}^{\bullet}) + H(\mathrm{H}^{+}) - H(\mathrm{ArOH}^{+\bullet}) \quad (10)$$

For this purpose, the enthalpies of the parent molecule, its free radicals in the positions 3' and 4', anions in the positions 3' and 4', and radical cation were calculated at the MN12-SX/6-311++G(d,p) level of theory. The enthalpy values of the solvated proton and electron in benzene (−898.7 and −14.4 kJ mol$^{-1}$), methanol (−1064.6 and −78.3 kJ mol$^{-1}$), and water (−1052.7 and −98.8 kJ mol$^{-1}$) were taken from literature.[30] The calculated reaction enthalpies are collected in Table 3. By comparing these enthalpies one can suppose which antioxidative mechanism of the **5CQA** prevails. Namely, the mechanism which is characterized with the smallest value of the reaction enthalpy is supposed to be the operative reaction pathway.

**Table 3.** Thermodynamic parameters (kJ mol$^{-1}$) related to the antioxidative mechanisms of chlorogenic acid in three different media in the positions 3' and 4'. The results obtained for the position 4' are given in the italic font

| | | Benzene | Methanol | Water |
|---|---|---|---|---|
| HAT | BDE | 344.1 | 346.5 | 346.6 |
| | | *333.0* | *335.5* | *335.6* |
| SPLET | PA | 350.2 | 119.8 | 128.8 |
| | | *329.4* | *104.0* | *113.2* |
| | ETE | 376.2 | 379.1 | 361.7 |
| | | *386.0* | *384.0* | *366.3* |
| SET-PT | IP | 656.8 | 515.8 | 491.8 |
| | PDE | 69.6 | -16.9 | -1.4 |
| | | *58.5* | *-27.9* | *-12.3* |

A careful inspection of Table 3 shows that **5CQA** will not obey SET-PT mechanism in any solvent, due to the highly endothermic first step of this mechanism. As expected, the BDE values in all three solvents are mutually very similar, indicating that the HAT mechanism is almost independent on the solvent polarity. In benzene the PA and ETE values are larger than the BDE values, so one can assume that the HAT mechanism will be predominant in nonpolar solvents. In polar solvents the PA values are smaller than the BDEs, while the ETE values are larger, but still comparable to the BDE values. Thus, one can suppose that the HAT and SPLET mechanisms are competitive in polar solvents. All these results are in excellent agreement with our previous findings obtained by employing the B3LYP-D2/6-311++G(d,p) and M06-2X/6-311++G(d,p) theoretical models,[22] thus indicating very similar performances of the three functionals in the thermodynamic investigations of antioxidative activity.

## CONCLUSIONS

The performance of the MN12-SX functional in the investigations of the structural, spectroscopic, and antioxidative properties of **5CQA** was examined and compared to those of the B3LYP-D2, B3LYP-D3, and M06-2X methods. In the simulated UV-vis spectrum the band at 329 nm was excellently reproduced, but the other three bands do not appear at all in the calculated spectrum. This fact indicates that MN12-SX is inferior to B3LYP-D3. However, this method is the best performer in reproducing the NMR spectra of **5CQA**. Capability of the tested

functional to reproduce the vibrational spectra, and to approximate thermodynamic quantities necessary for description of the antioxidative mechanisms, is comparable to those of other three methods.[21,22]

The MN12-SX calculations perfectly agree with previously revealed most stable conformations of **5CQA** in the gas phase[21] and solution.[17,21,22] The quinic moiety is characterized with directed hydrogen bonds, where the carboxylic hydrogen is not oriented towards the carbonyl oxygen of the carboxylic group, but towards the oxygen of the proximate hydroxyl group.

Thermodynamic approach to the investigation of the antioxidative action of **5CQA** showed that HAT may be the predominant mechanism in nonpolar solvents, while HAT and SPLET are competitive pathways in polar media. Mechanistic investigation of the HAT and SPLET reaction pathways are under intensive scrutiny.

**Acknowledgment.** This work was partially supported by the Ministry of Science and Technological Development of the Republic of Serbia (Grant no 172016), and bilateral project Serbia-Croatia 2016-2017.

## REFERENCES

[1] C. Clé, L. M. Hill, R. Niggeweg, C. R. Martin, Y. Guisez, E. Prinsen, M. A. Jansen, *Phytochemistry* **2008**, *69,* 2149.
[2] R. Niggeweg, A. J. Michael, C. Martin, *Nat. Biotechnol.* **2004,** *22,* 746.
[3] K. A. Leiss, F. Maltese, Y. H. Choi, R. Verpoorte, P. G. Klinkhamer, *Plant Physiol.* **2009**, *150*, 1567.
[4] Y. J. Liu, C. Y. Zhou, C. H. Qiu, X. M. Lu, Y. T. Wang, *Mol. Med. Rep.* **2013**, *8*, 1106.
[5] K. W. Ong, A. Hsu, B. K. Tan, *PLoS One* **2012**, *7*, e32718.
[6] A. Suzuki, N. Yamamoto, H. Jokura, M. Yamamoto, A. Fujii, I. Tokimitsu, I. Saito, *J. Hypertens.* **2006**, *24*, 1065.
[7] C. W. Wan, C. N. Wong, W. K. Pin, M. H. Wong, C. Y. Kwok, Y. C. Robbie, H. F. Y. Peter, C. Shun-Wan, *Phytother. Res.* **2013**, *27*, 545.
[8] K. W. Ong, A. Hsu, B. K. Tan, *Biochem. Pharmacol.* **2013**, *85*, 1341.
[9] J. G. Xu, Q. P. Hu, Y. Liu, *J. Agric. Food Chem.* **2012**, *60*, 11625.
[10] Y. Sato, S. Itagaki, T. Kurokawa, J. Ogura, M. Kobayashi, T. Hirano, M. Sugawara, K. Iseki, *Int. J. Pharm.* **2011**, *403*, 136.
[11] J. S. Wright, E. R. Johnson, G. A. DiLabio, *J. Am. Chem. Soc.* **2001**, *123*, 1173.
[12] E. Klein, V. Lukeš, M. Ilčin, *Chem. Phys.* **2007**, *336*, 51.
[13] G. Litwinienko, K. U. Ingold, *Accounts Chem. Res.* **2007**, *40*, 222.
[14] A. Galano, G. Mazzone, R. Alvarez-Diduk, T. Marino, J. R. Alvarez-Idaboy, N. Russo, *Annu. Rev. Food Sci. Technol.* **2016**, *7,* 335.
[15] G. F. Pauli, U. Kuczkowiaky, A. Nahrstedt, *Magn. Reson. Chem.* **1999**, *37*, 827.
[16] U. H. Jin, J. Y. Lee, S. K. Kang, J. K. Kim, W. H. Park, J. G. Kim, S. K. Moon, C. H. Kim, *Life Sci.* **2005**, *77*, 2760.
[17] M. Forino, G. C. Tenore, L. Tartaglione, C. Dell'Aversano, N. Novellino, P. Ciminiello, *Food Chem.* 2015, *178*, 306.
[18] P. J. Eravuchira, R. M. El-Abassy, S. Deshpande, M. F. Matei, S. Mishra, P. Tandon, N. Kuhnert, A. Materny, *Vib. Spectrosc.* **2012**, *61*, 10.
[19] J. P. Cornard, C. Lapouge, L. Dangleterre, C. Allet-Bodelot, *J. Phys. Chem. A* **2008**, *112*, 12475.
[20] M. Andjelković, J. V. Camp, B. De Meulenaer, G. Depaemelaere, C. Socaciu, M. Verloo, R. Verhe, *Food Chem.* **2006**, *98*, 23–31.
[21] S. Marković, J. Tošović, J. M. Dimitrić Marković, *Spectrochim. Acta A* **2016**, *164*, 67.
[22] S. Marković, J. Tošović, *Food Chem.* **2016**, *210*, 585.
[23] R. Peverati, D. G. Truhlar, *Phys. Chem. Chem. Phys.* **2012**, *14*, 16187.
[24] M. Cossi, N. Rega, G. Scalmani, V. Barone, *J. Comput. Chem.* **2003**, *24*, 669.
[25] R. A. Munos, Y. N. Panchenko, G. S. Koptev, N. F. Stepanov, *J. Appl. Spectrosc.* **1970**, *12*, 428.
[26] M. H. Jamróz, VEDA 4 Warsaw **2004**.
[27] M. J. Frisch, G. W. Trucks, H. B. Schlegel, G. E. Scuseria, M. A. Robb, J. R. Cheeseman, G. Scalmani, V. Barone, B. Mennucci, G. A. Petersson, H. Nakatsuji, M. Caricato, X. Li, H. P. Hratchian, A. F. Izmaylov, J. Bloino, G. Zheng, J. L. Sonnenberg, M. Hada, M. Ehara, K. Toyota, R. Fukuda, J. Hasegawa, M. Ishida, T. Nakajima, Y. Honda, O. Kitao, H. Nakai, T. Vreven, J. A. Montgomery, Jr., J. E. Peralta, F. Ogliaro, M. Bearpark, J. J. Heyd, E. Brothers, K. N. Kudin, V. N. Staroverov, R. Kobayashi, J. Normand, K. Raghavachari, A. Rendell, J. C. Burant, S. S. Iyengar, J. Tomasi, M. Cossi, N. Rega, J. M. Millam, M. Klene, J. E. Knox, J. B. Cross, V. Bakken, C. Adamo, J. Jaramillo, R. Gomperts, R. E. Stratmann, O. Yazyev, A. J. Austin, R. Cammi, C. Pomelli, J. W. Ochterski, R. L. Martin, K. Morokuma, V. G. Zakrzewski, G. A. Voth, P. Salvador, J. J. Dannenberg, S. Dapprich, A. D. Daniels, Ö. Farkas, J. B. Foresman, J. V. Ortiz, J. Cioslowski, D. J. Fox, Gaussian 09, Revision D.1, Gaussian Inc., Wallingford CT, **2013**.
[28] J. P. Merrick, D. Moran, L. Radom, *J. Phys. Chem. A* **2007**, *111*, 11683.
[29] S. Marković, J. Tošović, *J. Phys. Chem. A* **2015**, *119*, 9352.
[30] Z. Marković, J. Tošović, D. Milenković, S. Marković, *Comput. Theor. Chem.* **2016,** *178*, 11.